Metallophysics and Advanced Technologies
Металофіз. новітні технол.
Metallofiz. Noveishie Tekhnol.
2025, vol. 47, No. 6, pp. 567–573
https://doi.org/10.15407/mfint.47.06.0567
Reprints available directly from the publisher

PACS numbers: 61.46.Df, 61.80.Ed, 68.35.Ct, 68.37.Ps, 68.55.J-, 81.70.Pg

Morphological Properties of Manganese Ferrite Nanoparticles

A. F. Gochuyeva

Azerbaijan State Oil and Industry University,
20 Azadlig Ave.,
AZ-1010 Baku, Azerbaijan

The paper discusses the results for the sample with a high degree of purity (nanopowder with true density of 4.96 g/cm^3, particle size of 60 nm and purity of 98.5%; SkySpring Nanomaterials, USA) and, in comparison with it, prepared one in the form of a pill of size 4×15×5 mm for 1 hour; the surface morphology of the irradiated sample under the influence of γ-rays is studied. The AFM (atomic force microscopy) results show that the phases included in the composition of the ordinary $MnFe_2O_4$ nanoparticle are compactly assembled into different parts, and the presence of slight surface roughness is observed. In the irradiated sample, the phases are evenly distributed, and the surface roughness is clearly visible.

Key words: manganese ferrite, nanoparticles, γ-rays, surface morphology, AFM.

У статті обговорюються результати стосовно зразка високого ступеня чистоти (нанопорошок зі справжньою густиною у 4,96 г/см^3, розміром частинок у 60 нм і чистотою у 98,5%; SkySpring Nanomaterials, США) і, в порівнянні з ним, приготованого у формі пігулки розміром 4×15×5 мм упродовж 1 години; досліджено морфологію поверхні опроміненого зразка під впливом γ-променів. Результати АСМ (атомно-силової мікроскопії) показують, що фази, які входять до складу звичайної наночастинки $MnFe_2O_4$, компактно зібрані в різні частини; також спостерігається наявність невеликої шерсткости поверхні. В опроміненому зразку фази розподілені рів-

Corresponding author: Aynura F. Gochuyeva
E-mail: aynuragochuyeva@gmail.com

Citation: A. F. Gochuyeva, Morphological Properties of Manganese Ferrite Nanoparticles, *Metallofiz. Noveishie Tekhnol.*, **47**, No. 6: 567–573 (2025); DOI: 10.15407/mfint.47.06.0567

номірно, та чітко видно шерсткість поверхні.

Ключові слова: ферит Манґану, наночастинки, γ-промені, морфологія поверхні, АСМ.

(Received 13 August, 2024; in final version, 4 June, 2025)

1. INTRODUCTION

As we know, compared to large-scale materials and microparticles, nanoparticles exhibit more sophisticated and greater properties and enable their application in a large number of different fields. As a key member of the ferrite family, $MnFe_2O_4$ has been the subject of extensive research due to its special magnetic and electromagnetic properties. Understanding the magnetic properties of nanoparticles in magnetic materials is one of the important topics. The magnetic transitions present in nanostructured $MnFe_2O_4$ oxides with a spinel ferrite structure are widely used in industrial and medical biology. This nanoparticle is also a non-toxic compound and an environmentally friendly non-corrosive material, resistant to high temperature and impact. In $MnFe_2O_4$, about 80% of the Mn^{2+} ions are in the tetrahedral site and 20% in the octahedral site, so it is a partially inverted spinel. Spinel ferrites have the structure AB_2O_4, where A and B represent the tetrahedral and octahedral cation sites, respectively, and O represents the oxygen anion site. In the normal spinel structure, site A is occupied by Fe^{3+} ions, and in the reverse spinel structure, site A is occupied by Mn^{2+} ions. It is possible to control the shape and particle size of the $MnFe_2O_4$ compound, as well as adjust the catalytic, magnetic, dielectric, electronic, optical and electrical properties [1, 2]. By adding certain cations or anions to change the concentration of electrons and holes, the magnetic, optical and electrical properties of ferrites can be improved or adjusted. Spinel-containing ferrites have several advantages over inverse spinel ferrites, in part because they are cheaper, easier to manufacture, and have different magnetic properties. Furthermore, the radius, charge, lattice energy and crystal site stabilization energy of the solute ion added in sites A and B significantly affect the distribution of cations. Manganese ferrite ($MnFe_2O_4$) nanoparticles, which belong to spinel ferrites, are used in magnetic applications, such as recording media devices, drug delivery, ferrofluids, biosensors and contrast enhancement agents for MRI technology. There are many experimental synthesis methods to obtain $MnFe_2O_4$ ferrites. Among them, thermal decomposition, sol–gel, colloidal emulsion, solvo/hydrothermal and laser pyrolysis, *etc.* methods can be shown. Solvo/hydrothermal synthesis is an environmentally friendly approach to produce small and uniformly distributed nanostructures. It also makes

it easy to add particles to create composite materials [11]. The solvothermal synthesis method, usually obtained using a microwave oven, allows precise control of the parameters of compound properties, phase purity, high productivity, reproducibility, uniform particle morphology. Manganese ferrites at the nanoscale exhibit interesting morphological characteristics. Considering these and other characteristics, it can be assumed that manganese ferrite nanoparticles can be used in elements used in telecommunications by forming a composite with the polymer materials used in our previous work [3–10]. They have a wide range of applications ranging from fundamental research to industrial applications. In the present study, the surface morphology of ferrite nanoparticles was investigated.

2. EXPERIMENTAL DETAILS

Nanopowder sample with a true density of 4.96 g/cm^3, a particle size of 60 nm and a purity of 99.95% (SkySpring Nanomaterials, USA) was used during the studies. The $MnFe_2O_4$ nanoparticle has a spherical shape depending on the synthesis process. These particles in powder form are manufactured by pressing. Pressing process Model No. FTIR hydraulic press with ATHP-15 is made. The process was carried out under complete laboratory conditions. To do this, the nanoparticle in powder form is poured into a special mold of 4 mm wide, 15 mm long and 5 mm high and pressed at room temperature to form a pill. The pressure during pressing was 50 kg/cm^2. The samples obtained in the form of pills were irradiated with a gamma ray with a radiation power of $\dot{D} = 1.41$ gray/sec and a radiation dose of 50 gray. Nanoeducator, Scanning probe microscope (Northern Ireland), AFM (atomic force microscopy) also studied the surface morphology of the sample at the nanoscale.

3. RESULTS AND DISCUSSION

In our research, atomic force microscopy (AFM) of a nanoparticulate antiferromanganese-based sample was studied. Despite the wide application of AFM in materials science and its scientific and engineering impact, atomic force microscopy has been rarely used in magnetic nanoparticles. When doping is performed on various samples, TEM, SEM, *etc.* are used when studying their structure. It is very suitable to learn AFM analysis at the same time as analysis. In our work, the AFM images of the pure $MnFe_2O_4$ nanoparticle and pellet of size 4×15×5 mm prepared and irradiated under the influence of gamma rays for 1 hour were examined. The surface morphology, topology and coating thickness of the $MnFe_2O_4$ composite elements were determined using AFM

images. The AFM images were taken at 24°C, being stable and reproducible. Figure 1(*a*) shows a topographical image of a typical contact mode AFM top view of a $MnFe_2O_4$ nanoparticle. The nanoparticles with a spherical diameter of 60 nm are irregularly distributed in the thin layer. In Figure 1(*b*), a large number of bumps are observed on the surface of the joint, indicating that this feature belongs, for example, to $MnFe_2O_4$, a magnetic nanoparticle. In some areas, a compact agglomeration of magnetic particles caused by strong attraction between nanoparticles can be observed [12, 13].

Figure 1(*c*) shows the AFM image of the same point in front three-dimensional topographic format, *i.e.*, 3*D*. At 24°C, a few particles of a nanoparticle size mentioned above mixed with medium-size particles form a relatively irregular surface with a given and increasing roughness. Looking at a 3*D* topographic image, we see many protrusions that break up the flat surface, causing roughness. Moreover, as shown in the 2*D* and 3*D* topographic images of $MnFe_2O_4$, it is clear that the thickness increases due to the precipitation of Mn^+ ions in the ferrites, which increase the thickness with the increase of the coating layer. The morphological study shows that the thickness of the coating increases due to the accumulation of particles in the surface layers. Figure 1(*d*)

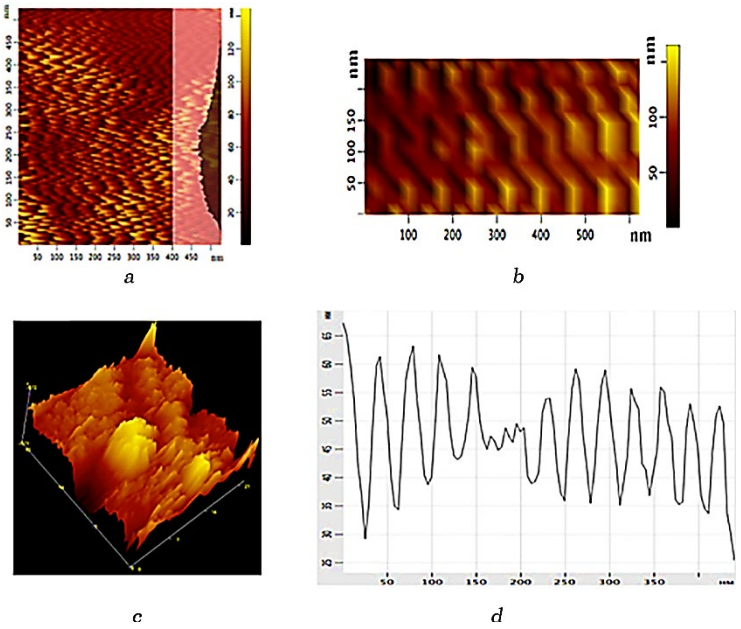

Fig. 1. *a*) typical topographic AFM image of a $MnFe_2O_4$ nanoparticle (in contact mode), *b*) 2*D* topographic image of a nanoparticle, *c*) 3*D* topographic image of a nanoparticle, *d*) height histogram of a nanoparticle obtained from data from a scanned surface 3×3 μm^2.

shows a histogram of the height size distribution of a $MnFe_2O_4$ nanoparticle obtained from data of a scanned area of 3×3 μm^2. This figure shows the elevation of the cross section produced by the irregular surface, which causes the roughness associated with the typical topographic image of a nanoparticle. From the data of the 3×3 μm^2 scanned area of the $MnFe_2O_4$ nanoparticle, it can be observed that the total surface roughness is approximately 67 nm [14, 15].

Figure 2(*a*) shows AFM images of a sample of $MnFe_2O_4$ nanoparticles prepared as 4×15×5 mm pellets and irradiated under the influence of γ-rays for 1 hour. Here, there is a topographic image of the AFM in contact mode. According to the topographic image, the crystal phases of the sample irradiated under the influence of γ-rays for 1 hour are distributed more evenly, and it is proven that the crystal phase is better. Spherical nanoparticles with a diameter of 60 nm are regularly distributed in the thin layer. Figure 2(*b*) shows that the phases are regularly distributed on the surface of the $MnFe_2O_4$ composite, unlike the 2*D* topographic image of the unirradiated sample. In the topographic image of the sample irradiated under the influence of γ-rays, the re-

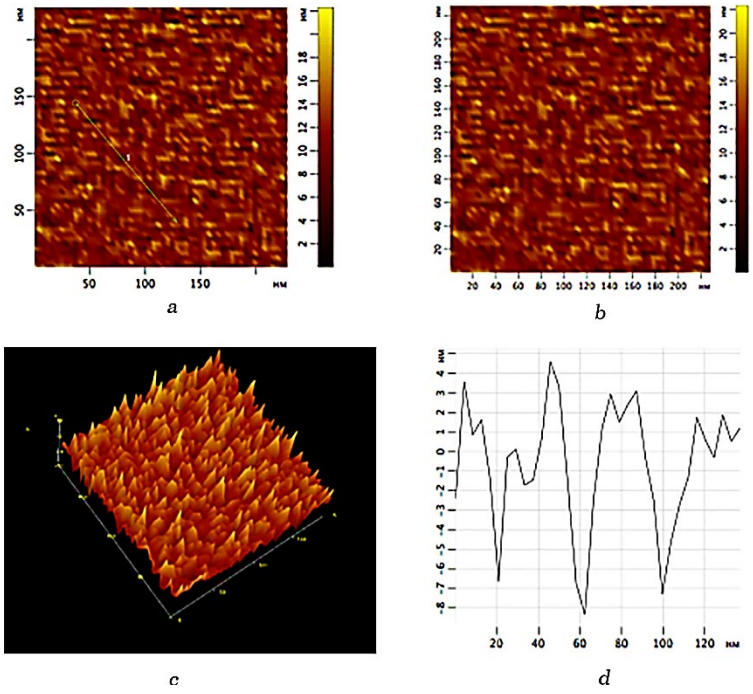

Fig. 2. *a*) typical AFM topographic image (in contact mode), *b*) 2*D* topographic image, *c*) 3*D* topographic image, *d*) height histogram obtained from data of a 3×3 μm^2 scanned area of a sample irradiated under the influence of γ-rays for 1 hour.

verse agglomeration process occurs in the entire area, *i.e.*, due to the lack of attraction between the nanoparticles, compact aggregation of the nanoparticles is not observed. The reason for this may be that the magnetic moment of the substance takes on an average value, depending on the valence of iron oxides (Fe^{2+} and Fe^{3+}) and also due to the effect of the given temperature during pressing.

Figure 2(*c*) shows the three-dimensional topographical image before AFM, *i.e.*, 3*D*, of the same point of the sample irradiated under the influence of γ-rays for 1 hour. Looking at the 3*D* topographic image, we see that the sample surface consists of roughness, which leads to an irregular layer. Even the roughness created along the surface appears in a regular form in terms of appearance. As shown in the two topographic images, the thickness also increased due to the precipitation of Mn^{+} ions in the ferrites, which increased the thickness with the increase of the coating layer. Figure 2(*d*) shows a histogram of the height size distribution obtained from data of a 3×3 μm^2 scanned area of a sample irradiated under the influence of γ-rays for 1 hour. This figure shows the elevation of the cross section produced by the irregular surface, which causes the roughness associated with the typical topographic image of a nanoparticle. From the data of the 3×3 μm^2 scanned area of the $MnFe_2O_4$ nanoparticle, it can be observed that the total surface roughness is approximately 4.7 nm.

4. CONCLUSIONS

In our research work, the necessary data for the important characteristics of the $MnFe_2O_4$ nanoparticle and the sample prepared in pill form of the above-mentioned size and subjected to the influence of gamma rays by AFM were presented. It was shown the similarities and differences observed in the polydispersity parameters obtained from the AFM data of the $MnFe_2O_4$ nanoparticle and the gamma-irradiated sample prepared as a pellet. As can be seen, the agglomeration process is clearly manifested on the surface of an ordinary nanoparticle. In the irradiated sample, no compact agglomeration is observed; on the contrary, the individual phases of the compound are arranged in an orderly manner. The reason for this regularity may be due to changes in valence of ferrite oxide.

REFERENCES

1. A. F. Gochuyeva, *J. Mod. Phys. B*, **36**, No. 2: 2150542 (2022).
2. A. F. Gochuyeva, *J. Mod. Phys. B*, **37**, No. 10: 350057 (2023).
3. M. A. Kurbanov, G. Z. Suleymanov, N. A. Safarov, A. F. Gochuyeva, I. N. Orujov, and Z. M. Mamedova, *Semicond.*, **45**: 503 (2011).
4. A. F. Gochuyeva, M. A. Kurbanov, B. H. Khudayarov, and A. M. Aliyeva, *Dig.*

J. Nanomater. Biostruct., **13**, No. 1: 185 (2018).
5. Z. M. Mammadova, M. A. Gurbanov, A. F. Gochuyeva, G. Z. Suleymanov, and D. B. Taghiyev, *EUFH*, No. 11, Section 13: 108 (2014).
6. A. F. Gochuyeva and Kh. Kh. Hashimov, *NMC&A*, **7**, No. 3: 194 (2023).
7. G. Z. Suleymanov, M. A. Gurbanov, A. Kh. Akbarov, Z. M. Mammadova, and A. F. Gochuyeva, *Azerbaijan Chem. J.*, No. 4: 50 (2017).
8. M. K. Kerimov, M. A. Kurbanov, A. A. Bayramov, N. A. Safarov, and A. F. Gochuyeva, *J. Scientific Israel – Technological Advantages*, **14**, No. 4: 9 (2012).
9. A. F. Gochuyeva, A. M. Mehdiyeva, and S. V. Bakhshaliyeva, *NMC&A*, **8**, No. 1: 87 (2024).
10. A. F. Gochuyeva, Kh. Kh. Hashimov, and I. Y. Bayramov, *Chalcogenide Lett.*, **20**, No. 4: 285 (2023).
11. A. F. Gochuyeva, *Semicond. Phys. Quantum Electron. Optoelectron.*, **27**, No. 3: 298 (2024).
12. S. H. Hosseini, R. Rahimi, and H. Kerdari, *Polym. J.*, **43**: 745 (2011).
13. L. P. Silva, Z. G. M. Lacava, N. Buske, P. C. Morais, and R. B. Azevedo, *J. Nanoparticle Res.*, **6**: 209 (2004).
14. Y. Yan, F. Shu, H. Chen, Zh. Dun, W. Lv, Zh. Zhang, W. Sun, and M. Liu, *Adv. Mater. Interfaces*, **10** (2023).
15. S.-K. Tong, P.-W. Chi, S.-H. Kung, and D.-H. Wei, *Sci. Rep.*, **8**: 1338 (2018).